



HHS Public Access

Author manuscript

Gene Ther. Author manuscript; available in PMC 2011 February 01.

Published in final edited form as:

Gene Ther. 2010 August ; 17(8): 1042–1051. doi:10.1038/gt.2010.87.

AAVrh.10-mediated Genetic Delivery of Bevacizumab to the Pleura to Provide Local Anti-VEGF to Suppress Growth of Metastatic Lung Tumors

Masaki Watanabe, Julie L. Boyer, and Ronald G. Crystal

Department of Genetic Medicine, Weill Cornell Medical College, New York, New York

Summary

Vascular endothelial growth factor (VEGF) produced by tumor cells plays a central role in stimulating angiogenesis required for tumor growth. Humanized monoclonal anti-VEGF antibody (bevacizumab, Avastin[®]), approved as a treatment for non-squamous, non-small cell lung cancer, requires administration every 3 wk. We hypothesized that an intrapleural administration of an adeno-associated virus (AAV) vector expressing an anti-VEGF-A antibody equivalent of bevacizumab would result in sustained anti-VEGF-A localized expression within the lung and suppress metastatic tumor growth. The AAV vector AAVrh.10 α VEGF encodes the light chain and heavy chain cDNAs of monoclonal antibody A.4.6.1, a murine antibody that specifically recognizes human VEGF-A with the same antigen-binding site as bevacizumab. A metastatic lung tumor model was established in SCID mice by intravenous administration of human DU145 prostate carcinoma cells. Intrapleural administration of AAVrh.10 α VEGF directed long term expression of the anti-human VEGF-A antibody in lung, as demonstrated by sustained, high level anti-human VEGF titers in lung epithelial lining fluid for 40 wk, the duration of the study. In the AAVrh.10 α VEGF-treated animals, tumor growth was significantly suppressed ($p < 0.05$), the numbers of blood vessels and mitotic nuclei in the tumor was decreased ($p < 0.05$), and there was increased survival ($p < 0.05$). Thus, intrapleural administration of an AAVrh.10 vector encoding a murine monoclonal antibody equivalent of bevacizumab, effectively suppresses the growth of metastatic lung tumors, suggesting AAV-mediated gene transfer to the pleura to deliver bevacizumab locally to the lung as a novel alternative platform to conventional monoclonal antibody therapy.

Introduction

Lung cancer is the leading cause of cancer-related deaths for both men and women. An estimated 219,000 new diagnoses and 159,000 deaths are expected from lung cancer in the United States in 2009¹. The prognosis is poor with the majority of advanced non-small cell lung cancer patients dying in less than a year despite the use of various combination chemotherapy^{2–8}.

Users may view, print, copy, download and text and data- mine the content in such documents, for the purposes of academic research, subject always to the full Conditions of use: http://www.nature.com/authors/editorial_policies/license.html#terms

Correspondence: Department of Genetic Medicine, Weill Cornell Medical College, 1300 York Avenue, Box 96, New York, New York 10065, Phone: (646) 962-4363, Fax: (646) 962-0220, geneticmedicine@med.cornell.edu.

Tumors produce mediators of angiogenesis to induce the ingrowth of vasculature from local tissues, facilitating the delivery of oxygen and nutrients to the proliferating tumor cells⁹. Vascular endothelial growth factor (VEGF) is the key- proangiogenic factor, necessary for the development of novel vessels in tumors¹⁰⁻¹⁵. Bevacizumab (Avastin[®]) is a humanized IgG1 monoclonal antibody specific for VEGF-A, the major form of VEGF produced by human^{16,17}. Bevacizumab binds to all VEGF-A isoforms, and prevents VEGF-A from activating the two major VEGF receptors, VEGFR-1 (flt-1) and VEGFR-2 (KDR)^{16,17}. In immunodeficient mice, bevacizumab inhibits the growth of human tumor cell lines that express VEGF-A¹⁸⁻²¹. In humans, bevacizumab prolongs the time to progression in several cancers, including lung cancer²²⁻²⁶. The U.S. Food and Drug administration (FDA) approved bevacizumab as a treatment for unresectable, locally advanced, recurrent or metastatic non-squamous, non-small cell lung cancer. The recommended dosage for lung cancer is 15 mg/kg every 3 wk. (<http://www.avastin.com/avastin/index.jsp>).

With the goal of developing a alternative platform for delivering bevacizumab to the lung, we hypothesized that an intrapleural administration of an adeno-associated virus (AAV) vector expressing an anti-VEGF-A antibody equivalent of bevacizumab would result in sustained anti-VEGF-A antibody delivery in the lung and suppress the growth of metastatic lung tumor. To assess this, we used an adeno-associated viral gene transfer vector (AAVrh.10 α VEGF) expressing the heavy and light chains of a monoclonal antibody with a human VEGF-A antigen recognition site identical to bevacizumab^{21,27}. The data demonstrates that a single intrapleural administration of AAVrh.10 α VEGF directs the long term expression of anti-human VEGF-A antibody in lung and suppresses the vascularity and proliferation of metastatic lung tumors, with concomitant suppression of the growth of the tumors and increases survival of the tumor-bearing mice.

Methods

Adeno-associated Virus Vectors

All AAV vectors were based on the nonhuman primate-derived AAV serotype rh.10 capsid with the AAV serotype 2 5' and 3' inverted terminal repeats and the transgene under the control of the cytomegalovirus (CMV) promoter. AAVrh.10 α VEGF encodes the anti-human VEGF light chain and heavy chain sequence separated by a poliovirus internal ribosome entry site (IRES) to facilitate expression of both protein subunits from a single promoter^{21,27}. The expression cassette in the AAVrh.10 α VEGF vector contains (5' to 3') the CMV promoter, the anti-human VEGF light chain-coding sequence, the poliovirus IRES, the anti-human VEGF heavy chain-coding sequence and the simian virus 40 polyadenylation signal. Synthetic antibody heavy and light chain variable domains selected for the study were derived from the protein sequence for antibody A.4.6.1, the murine antibody that was humanized to generate bevacizumab²⁸. The coding sequences for the human VEGF-A binding site are identical to that of bevacizumab²⁹. The variable domains were incorporated into full-length heavy and light chains by adding the murine IgG1 constant domain and the murine κ constant domain onto the variable regions by overlap polymerase chain reaction (PCR).

AAVrh.10 α VEGF was produced using three plasmids: (1) pAAV α VEGFab, an expression plasmid containing (5' to 3') the AAV2 5'-inverted terminal repeat including packaging signal (ψ), the anti-human VEGF antibody expression cassette, and the AAV2 3'-inverted terminal repeat; (2) pAAV44.2, a packaging plasmid that provides the AAV Rep proteins derived from AAV2 needed for vector replication and the viral structural (Cap) proteins VP1, 2 and 3 derived from AAVrh.10, which determine the serotype of the AAV vector; and (3) pAdDeltaF6, an Ad helper plasmid that provides Ad helper functions of E2, E4 and VA RNA³⁰⁻³³. For AAVrh.10 vector production, pAAV α VEGF (600 μ g), pAAV44.2 (600 μ g) and pAdDeltaF6 (1.2 mg) were co-transfected into human embryonic kidney 293 cells (American Type Culture Collection, Manassas, VA), which contains an integrated copy of the Ad E1 region, using Polyfect (Qiagen, Valencia, CA). At 72 hr after transfection, the cells were harvested, a crude viral lysate was prepared using 4 cycles of freeze/thaw, and clarified by centrifugation. AAVrh.10 α VEGF was purified by iodixanol gradient and QHP anion exchange chromatography. The purified AAVrh.10 α VEGF was concentrated using an Amicon Ultra-15 100K centrifugal filter devices (Millipore, Billerica, MA) and stored in phosphate-buffered saline, pH 7.4 (PBS) at -80°C . The negative control vector, AAVrh.10 α PA, encodes an unrelated antibody against anthrax protective antigen³⁴, and AAVrh.10EGFP encodes variant of wild-type green fluorescent protein. Vector genome titers were determined by quantitative TaqMan real-time PCR analysis using a CMV promoter-specific primer-probe set (Applied Biosystems, Foster City, CA)³³.

Assessment of AAVrh.10 α VEGFab *In Vitro*

Expression and specificity of the anti-human VEGF-A antibody from AAVrh.10 α VEGF after infection of cells *in vitro* was assessed by Western analysis. 293orf6 cells, from a human embryonic kidney cell line expressing Ad E1 and E4 genes were infected with AAVrh.10 α VEGF (2×10^5 genome copies, gc/cell) and infected-cell supernatants were harvested 72 hr postinfection. Supernatants were concentrated by passage through Ultracel YM-10 centrifugal filters (Millipore, Billerica, MA) and evaluated for the expression of anti-human VEGF-A antibody by Western analysis under reducing conditions, using a peroxidase-conjugated sheep anti-mouse IgG secondary antibody (SIGMA, Saint Louis, MO) and enhanced chemiluminescence (ECL) reagent (GE Healthcare Life Sciences, Piscataway, NJ). The specificity of the AAVrh.10-expressed anti-VEGF antibody for human VEGF was determined by Western analysis with human VEGF-A121 and VEGF-A165 or with mouse VEGF-A120 and VEGF-A164 as the target antigens and infected cell supernatants as the primary antibody. Detection was with a peroxidase-conjugated anti-mouse IgG secondary antibody (SIGMA) and ECL reagent (GE Healthcare Life Sciences).

Anti-VEGF-A Antibody Levels After Local Administration of AAVrh.10 α VEGF

Male C57BL/6 mice, 8 to 10 weeks of age, obtained from The Jackson Laboratory (Bar Harbor, ME) or Taconic (Germantown, NY), were housed under pathogen-free conditions. To determine which local administration route of the AAVrh.10 α VEGF vector would deliver the highest levels of the anti-VEGF-A antibodies to the lung, AAVrh.10 α VEGF (10^{11} gc) in 100 μ l PBS was administered by the intrapleural or intratracheal routes to C57BL/6 mice. After 1 to 40 wk, lung epithelial lining fluid (ELF) and serum were collected. Lung ELF was collected by cannulating the trachea with 24-gauge angiocatheter

and flushing and aspirating three times with 500 μ l PBS, and then centrifuged at 3,500 rpm for 5 min. Blood was collected via the tail vein, allowed to clot for 60 min, and centrifuged at 13,000 rpm, 10 min. Anti-human VEGF-A antibody levels in lung ELF and serum were assessed by a human VEGF-specific enzyme-linked immunosorbent assay (ELISA) using flat bottomed 96-well EIA/RIA plates (Corning Life Sciences, Lowell, MA) coated with 0.1 μ g human VEGF-A165 per well in a total volume of 100 μ l of 0.05 M carbonate buffer containing 0.01% thimerosal overnight at 4°C. The plates were washed three times with PBS and blocked with 5% dry milk in PBS for 30 min. The plates were washed 3 times with PBS containing 0.05% Tween 20 (PBS-Tween). Serial lung ELF dilutions in PBS containing 1% dry milk were added to each well and incubated for 60 min. The plates were washed 3 times with PBS-Tween and 100 μ l/well of 1:10,000 diluted horseradish peroxidase conjugated goat anti-mouse IgG1 (Santa Cruz Biotechnology, Santa Cruz, CA) in PBS containing 1% dry milk was added and incubated for 60 min. The plates were washed 4 times with PBS-Tween and once with PBS. Peroxidase substrate (100 μ l/well; Bio-Rad, Hercules, CA) was added; after 10 min, the reaction was stopped by addition of 2% oxalic acid (100 μ l/well). Absorbance at 415 nm was measured. Antibody titers were calculated with a log (OD)-log (dilution) interpolation model and a cutoff value equal to 2-fold the absorbance of background.³⁵ The dilution of lung ELF with the PBS used for bronchoalveolar lavage (BAL) was corrected by the urea method³⁶. The urea concentration in bronchoalveolar lavage fluid (BALF) and serum was determined using quantichrom urea assay kit (Bioassay Systems, Hayward, CA). The lung ELF anti-VEGF-A antibody titer was calculated by the formula: Lung ELF anti-VEGF-A antibody titer = (BALF anti-VEGF-A antibody titer) \times (serum urea concentration)/(BALF urea concentration)^{36,37}. BALF total protein levels were measured using a bicinchoninic protein assay (Thermo Scientific) as specified by the manufacturer.

Organ Distribution of Anti-VEGF-A Antibody mRNA Expression Levels After Intrapleural AAVrh.10 α VEGF Administration

Quantitative TaqMan real-time polymerase chain reaction (PCR) analysis was used to evaluate organ distribution of anti-VEGF-A antibody mRNA expression levels after intrapleural AAVrh.10 α VEGF (10¹¹ gc) administration. Primers and probe to quantify anti-VEGF antibody mRNA levels were 5'-GGTCTTAAGTGGATGGGATGGA-3', 5'-TGTGAACCTGCGCTTGAAATC-3', and FAM-TAATACTTATACTGGAGAACCCTACCTACGCTG-TAMRA, respectively. Eighteen wk after vector administration, liver, diaphragm, lung, heart, spleen, and kidney were collected and total RNA was extracted with TRIzol (Invitrogen, Carlsbad, CA) followed by DNA digestion with deoxyribonuclease I, Amplification Grade (Invitrogen). First strand cDNA was synthesized from 1 μ g of total RNA in a 50 μ l reaction volume, using TaqMan reverse transcription reagents (Applied Biosystems, Foster City, CA) with random hexamers as primers for RT-PCR. Quantitative TaqMan real-time PCR relative to an 18S ribosomal RNA (rRNA) primer and probe set as the internal control (Applied Biosystems) was performed to assess the expression levels of anti-VEGF antibody mRNA in the sample, using the Ct method²⁷ with analysis at two RNA concentrations to demonstrate that amplification efficiency for rRNA reference and anti-VEF RNA was the same.

Metastatic Lung Tumor Therapy Model

Female non-obese diabetic/severe combined immunodeficient (NOD/SCID) mice, 8 to 10 wk of age, were obtained from The Jackson Laboratory (Bar Harbor, ME) or Taconic (Germantown, NY) and were housed under pathogen-free conditions. DU 145 prostate carcinoma cells (5×10^5 cells/mouse; American Type Culture Collection, Manassas, VA) in 100 μ l PBS were administered intravenously via left jugular vein. On the next day, the mice were treated by intrapleural administration of 10^{11} gc AAVrh.10 α VEGF in 100 μ l PBS or, as control vectors, AAVrh.10 α PA, AAVrh.10EGFP or PBS alone.

Histologic Analyses

To assess lung histopathology, animals that received AAVrh.10 α VEGF were sacrificed 18 wk after tumor administration. Samples from control groups that received AAVrh.10 α PA, AAVrh.10EGFP or PBS were collected when they died or were sacrificed due to morbidity by 18 wk. The lungs were inflated to total lung capacity with 4% paraformaldehyde injection via an angiocatheter placed in the trachea and tied with sutures. The inflated lungs were removed *en bloc* and fixed in 4% paraformaldehyde overnight. Gross photos were taken before paraffin embedding. Standard hematoxylin and eosin (H&E) staining was performed using the lungs sections (5 μ m). The number of blood vessels and mitotic nuclei in the metastatic tumors was quantified by immunohistochemical staining for vascular endothelial cells and nuclei. Sections were stained with goat anti-mouse vascular endothelial cadherin (VE-cadherin) antibody (R&D Systems, Minneapolis, MN) followed with biotin-conjugated anti-goat IgG antibody (Jackson ImmunoResearch, West Grove, PA) and peroxidase conjugated streptavidin with 3,3'-diaminobenzidine (DAB) for visualization. Nuclei were stained with hematoxylin or 4',6-diamidino-2-phenylindole (DAPI). For quantification of angiogenesis, the number of VE-cadherin positive vessels in 5 random 40x fields was counted in a blinded manner. The mitotic index was calculated as (number of nuclei in mitotic phase)/(total number of nuclei) in 5 random 60x fields.

Assessment of Metastatic Lung Tumor Volume

Tumor cells and AAV vectors were administered as described above. Sixteen wk after tumor cell administration, animals that received AAVrh.10 α VEGF were sacrificed and whole lungs were collected and weighed. Samples from control groups that received AAVrh.10 α PA, AAVrh.10EGFP or PBS were collected when they died or were sacrificed due to morbidity by 16 wk. Quantitative TaqMan real-time PCR analysis for Alu was used to quantify human DNA as a marker of human tumor volume in right lung. Genomic DNA was extracted with the DNeasy blood & tissue kit (Qiagen, Valencia, CA). Primers and probes for Alu sequences were 5'-CGGGTTCACGCCATTCTC-3', 5'-AAAAATTAGCCGGCGTAGTG-3', and FAM-AGCTGGGACTACAGGCGCCCG-TAMRA, respectively. For absolute quantification of the human DNA, a standard curve was generated using a serial dilution of purified human DNA. The amount of human DNA in mouse lung was normalized per total DNA.

Survival Study

Tumors and AAV vectors were administered as described above. When the mice died or were sacrificed due to morbidity, this was recorded as the date of death.

Statistical Analysis

All data are shown as mean \pm standard error. Statistical comparison was made by two-tailed Student t test, and a value of $p < 0.05$ was accepted as indicating significance. Survival evaluation was carried out by Kaplan-Meier analysis.

Results

In Vitro Characterization of AAVrh.10 α VEGF

To examine expression of the anti-VEGF-A antibody by AAVrh.10 α VEGF, 293orf6 cells were infected with AAVrh.10 α VEGF or as controls, uninfected or infected with AAVrh.10EGFP. Seventy-two hr post-infection, cell supernatants were collected and antibody expression was examined under reducing conditions (Figure 1A). Supernatants collected from AAVrh.10 α VEGF-infected cells (lane 3) demonstrated the presence of antibody heavy (50 kDa) and light (25 kDa) chains. No antibody was detected in mock or AAVrh.10EGFP-infected cells (lanes 1, 2).

The specificity of the AAV-expressed anti-VEGF-A antibody for human VEGF was assessed by Western analysis (Figure 1B). When bovine serum albumin (BSA), mouse VEGF-A120, mouse VEGF-A164, human VEGF-A121, and human VEGF-A165 proteins were probed with supernatants from AAVrh.10 α VEGF-infected cells, the anti-VEGF antibody recognized human VEGF-A but not bovine serum albumin or mouse VEGF-A (lanes 10–14). In contrast, supernatants from AAVrh.10EGFP-infected cells did not recognize either protein (lane 5–9). Thus, AAVrh.10 α VEGF expressed a full length antibody that has specificity for human VEGF-A.

Lung ELF and Serum Anti-VEGF-A Antibody Levels after Local Administration of AAVrh.10 α VEGF

To determine which local administration route of AAVrh.10 α VEGF would achieve the highest lung anti-VEGF-A antibody levels, lung ELF antibody levels were assessed 8 wk after intrapleural or intratracheal administration of the same dose (10^{11} gc) of the vector. Intrapleural administration of AAVrh.10 α VEGF resulted in high anti-VEGF-A antibody expression levels in lung ELF (Figure 2A; $p < 0.05$ compared with all other groups). No anti-VEGF-A antibody was detected in the lung ELF from mice that received intratracheal AAVrh.10 α VEGF, intrapleural AAVrh.10 α PA or intrapleural AAVrh.10EGFP. Assessment of the expression profile of anti-VEGF-A antibody in lung ELF and serum over 40 wk after intrapleural administration of AAVrh.10 α VEGF showed that antibody levels peaked at 4 and 8 wk, respectively, with a mild, then gradual decrease over a period of 24 wk, and then these levels were sustained throughout the 40 wk (Figure 2). Evaluation of BALF total protein levels as a marker of lung inflammation demonstrated no marked elevation after intrapleural administration of AAVrh.10 α VEGF compared to naive mice throughout a 40 wk time period [naïve at 40 wk, 477.5 ± 59.6 μ g/ml ($p > 0.4$ compared with all time points);

maximum level at 16 wk, 531.2 ± 46.7 $\mu\text{g/ml}$]. The data suggest that no significant lung inflammation was elicited during the experimental period by intrapleural AAVrh.10 α VEGF administration.

Organ Distribution of Anti-VEGF-A Antibody mRNA Expression Levels After Intrapleural AAVrh.10 α VEGF Administration

To evaluate the organ distribution of anti-VEGF-A antibody mRNA expression levels following intrapleural AAVrh.10 α VEGF administration, anti-VEGF-A antibody mRNA expression levels relative to endogenous 18S rRNA in various tissues were assessed by quantitative TaqMan real-time PCR. As expected from local administration in the pleura, anti-VEGF-A antibody mRNA was found in the diaphragm and the lung (Figure 3). Anti-VEGF-A antibody mRNA was undetectable in heart, liver, kidney or spleen. In a previous study, we similarly demonstrated that following intrapleural administration of AAVrh.10, the highest levels of transgene expression were found in thoracic structures, i.e., diaphragm, chest wall and heart³³.

Effects of Intrapleural AAVrh.10 α VEGFab Administration on Metastatic Lung Tumor Growth

To determine the effects of intrapleural AAVrh.10 α VEGF administration on metastatic lung tumor growth, lung histopathology, lung weight and human DNA expression levels in lung were assessed. Treatment with AAVrh.10 α VEGF resulted in a marked reduction of metastatic lung tumor growth as assessed by histology (Figure 4). The lung weight and human DNA expression levels in lung demonstrated a significant reduction in AAVrh.10 α VEGF-treated mice relative to animals that received PBS, AAVrh.10EGFP or AAVrh.10 α PA (Figure 5; $p < 0.05$, compared with all control treated groups and similar to naive animals, $P > 0.09$). These results indicate that the anti-VEGF-A antibody expressed from AAVrh.10 α VEGF was effective in suppressing growth of metastatic lung tumor in this xenograft model.

Effects of Intrapleural AAVrh.10 α VEGF Administration on Metastatic Lung Tumor Vascularization

To directly evaluate the effect of intrapleural AAVrh.10 α VEGF administration on angiogenesis in metastatic lung tumor, the number of blood vessels in tumors after AAVrh.10 α VEGF administration were quantified by immunohistochemistry for VE-cadherin, a surface marker on vascular endothelial cells. Immunohistochemical assessment demonstrated a marked reduction of vascularization in AAVrh.10 α VEGF-treated tumors as compared with PBS-, AAVrh.10EGFP- or AAVrh.10 α PA-treated tumors (Figure 6; $p < 0.05$, compared with all other controls). These data indicate a correlation between reduced tumor growth and a reduced number of blood vessels in AAVrh.10 α VEGF-treated mice.

Effects of Intrapleural AAVrh.10 α VEGF Administration on Metastatic Lung Tumor Proliferation

To evaluate the effect of intrapleural AAVrh.10 α VEGF administration on metastatic lung tumor proliferation, the number of nuclei in mitotic phase after AAVrh.10 α VEGF

administration was quantified by immunohistochemistry of tumor sections with DAPI (Figure 7A–D). Immunohistochemical assessment demonstrated a marked reduction of mitotic index in AAVrh.10 α VEGF-treated tumors as compared with the PBS-, AAVrh.10EGFP- or AAVrh.10 α PA-treated tumors. (Figure 7E; $p < 0.05$, compared with all other groups). These data indicate that reduced tumor growth results from a decrease not only in tumor vascularization, but in the number of dividing tumor cells.

Effects of Intrapleural AAVrh.10 α VEGF Administration on Survival of Metastatic Lung Tumor-bearing Mice

AAVrh.10 α VEGF-treated mice exhibited a statistically significant survival advantage in contrast to mice that received AAVrh.10 α PA, AAVrh.10EGFP or PBS (Figure 8; $p < 0.002$, AAVrh.10 α VEGF compared with all other groups).

Discussion

This study demonstrates that a single intrapleural administration of an AAV vector encoding the murine equivalent of bevacizumab is effective in directing long term expression of anti-VEGF-A antibody in lung, reducing metastatic lung tumor volume, the numbers of blood vessels and mitotic nuclei in the tumor, and in increasing survival of tumor-bearing mice. These observations suggest that AAV-mediated genetic modification of cells within an organ may be an effective strategy to generate local production of anti-angiogenesis monoclonal antibodies sufficient to protect that organ from the growth of metastatic lesions.

Bevacizumab (Avastin)

Bevacizumab binds specifically to all human VEGF isoforms, and prevents the binding of VEGF to its receptors with consequent inhibition of angiogenesis and tumor growth^{16,17}. In combination with standard chemotherapy, bevacizumab significantly prolongs the survival of patients with metastatic cancers of the colon, breast, kidney and lung^{22–26}. The efficacy of bevacizumab as a cancer therapy led to its approval by the FDA in 2006 as the first anti-angiogenic agent for the treatment of non-squamous, non-small cell lung cancer. Bevacizumab was derived from the murine anti-VEGF-A monoclonal antibody A.4.6.1^{18,28}. Humanization of A.4.6.1 to reduce immunogenicity and to increase half-life in humans resulted in an antibody molecule that is 93% human and 7% murine and retains the same biochemical and pharmacologic properties of the parental antibody¹⁸. Both antibodies effectively inhibit the growth of various human tumors *in vivo*³⁸. In previous studies, we demonstrated that adenovirus-mediated gene transfer of monoclonal antibody A.4.6.1 suppressed flank tumor growth²¹ and VEGF-induced high-permeability pulmonary edema²⁷, suggesting that genetic delivery of anti-VEGF-A antibodies may be a strategy to further increase antibody half-life and consequent bioavailability as an alternative to conventional monoclonal antibody therapy.

Genetic Delivery of Therapeutic Antibodies for Cancer

Genetic transfer of therapeutic antibodies is an effective strategy to achieve long-term persistence of antibody *in vivo*, and a consequently attractive strategy for cancer therapy. Antibody molecules have been expressed using a variety of viral vector systems and this

strategy has been demonstrated to have therapeutic effects against tumors in several experimental studies^{21,39-43}. We have previously demonstrated that adenovirus-based delivery of an anti-VEGF-A antibody with the equivalent antigen binding site of bevacizumab is effective in reducing tumor size, blood vessel density and tumor proliferation and in increasing survival of human tumor-bearing mice²¹. An adenovirus encoding the idiotype of a B cell lymphoma provided protection from subsequent tumor challenge in mice and prolonged the survival of mice with pre-existing tumors⁴⁰ and expression of an anti-HER-2 monoclonal antibody from an adenovirus vector resulted in detectable serum antibody levels for up to 4 wk after vector administration with; levels high enough to significantly reduce the growth of HER-2-positive tumor xenografts⁴². A recombinant vaccinia virus was engineered to express the heavy and light chains corresponding to the surface immunoglobulin of a malignant B cell, and immunized mice were protected against growth of tumorigenic cells expressing the same immunoglobulin³⁹. Stable antibody expression was observed for 4 months in nude mice using an AAV8 vector encoding a monoclonal antibody specific for the vascular endothelial growth factor receptor-2 (VEGFR2). This vector mediated a reduction of VEGFR2-positive tumor growth when tumor cells were introduced into the animals⁴¹. Finally, administration of an AAV1 vector expressing an anti-epidermal growth factor receptor antibody to muscle resulted in detectable serum antibody levels for 12 wk and suppression of established tumor growth⁴³.

AAV-mediated Transfer of Bevacizumab to the Pleura

In comparison with Ad vectors, AAV-based vectors direct long-term transgene expression with low toxicity⁴⁴. Although wild-type AAV can establish a latent infection by integrating into the host chromosome, integration of recombinant AAV vectors is inefficient, and the persistence of AAV gene delivery vectors in tissues is largely attributable to episomal genomes⁴⁵. AAV-mediated intracellular reporter gene transfer to the pleura results in high levels of transgene expression in thoracic structures^{33,46}. Intrapleural administration of an AAV5-based vector expressing human α 1-antitrypsin resulted in high levels of human α 1-antitrypsin in lung ELF.⁴⁶ A single administration of an AAVrh.10-based vector encoding an anthrax toxin-specific monoclonal antibody to the pleura mediated long-term serum antibody expression levels up to 26 wk and the protective effect against anthrax toxin persisted throughout the same time period³⁴. Genetic transfer of an anti-respiratory syncytial virus (RSV) antibody to the pleura with an AAVrh.10 vector resulted in protective anti-RSV neutralizing antibody activity in lung ELF for up to 23 wk⁴⁷. In the present study, intrapleural administration of AAVrh.10 α VEGF provides sustained anti-VEGF-A antibody expression levels in lung ELF for 40 wk (the duration of the study) after vector administration; this is in contrast to intrapleurally-administered adenovirus-based anti-VEGF, that did not result in anti-VEGF expression in a previous study²⁷. Quantitative analysis of tissue distribution of the anti-human VEGF-A antibody mRNA expression levels after intrapleural AAVrh.10 α VEGF administration demonstrated that the highest levels of transgene expression were in the chest structures (diaphragm and the lung), with no expression levels in the liver or spleen. Thus, intrapleural administration of AAV vectors can be used as a strategy to deliver therapeutic genes locally to the thoracic organs. Further, the pleura as a site for gene transfer has little risk of possible vector-induced inflammation since even marked pleural inflammation is not associated with lung dysfunction. This

concept is supported by the vast clinical experience of purposefully inducing inflammation in the pleura with sclerosing agent to seal the pleural space as therapy for malignant pleural effusion or recurrent pneumothorax^{48, 49}.

Taken together, the data obtained from the current study indicate that AAV-mediated genetic delivery of bevacizumab to the pleura to deliver locally to the lung represent a novel alternative approach to conventional monoclonal antibody therapy for metastatic lung cancer.

Acknowledgments

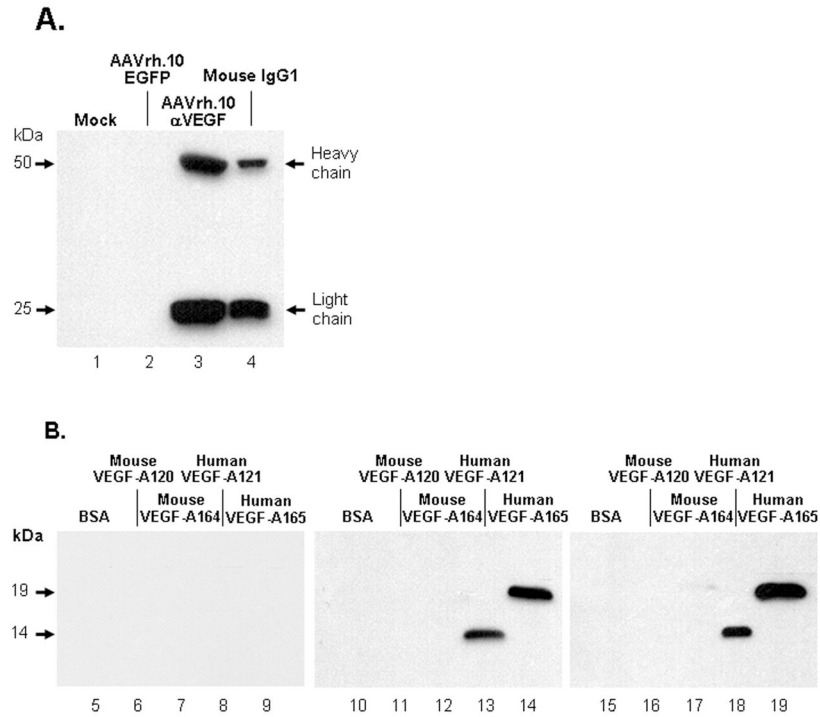
We thank Neil R. Hackett and Jasen Murray for help with quantitative TaqMan real-time PCR and Nahla Mohamed for help in preparing this manuscript. These studies were supported, in part, by U01 HL66952.

References

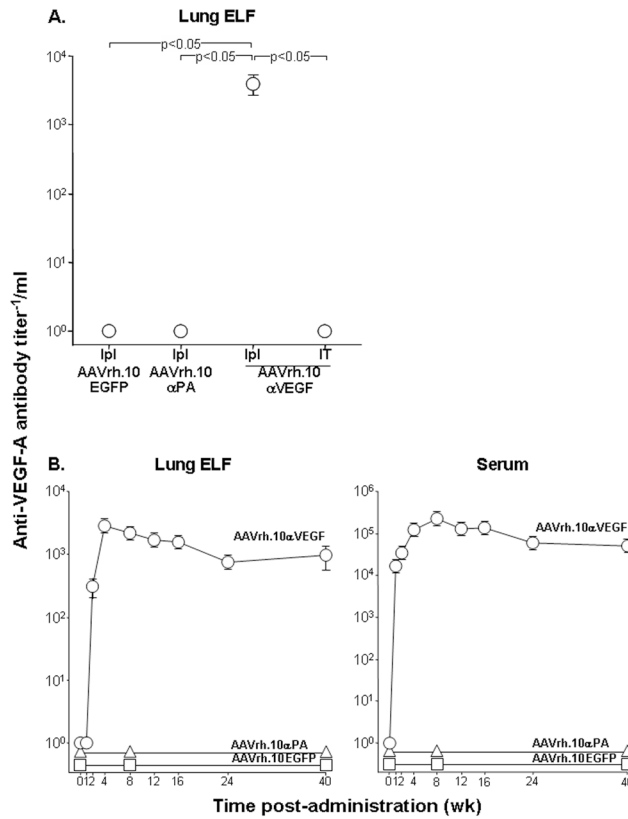
1. Jemal A, Siegel R, Ward E, Hao Y, Xu J, Thun MJ. Cancer Statistics, 2009. *CA Cancer J Clin*. 2009
2. Belani CP, Ramalingam S, Perry MC, LaRocca RV, Rinaldi D, Gable PS, et al. Randomized, phase III study of weekly paclitaxel in combination with carboplatin versus standard every-3-weeks administration of carboplatin and paclitaxel for patients with previously untreated advanced non-small-cell lung cancer. *J Clin Oncol*. 2008; 26:468–473. [PubMed: 18202422]
3. Blumenschein GR Jr, Khuri FR, von PJ, Gatzemeier U, Miller WH Jr, Jotte RM, et al. Phase III trial comparing carboplatin, paclitaxel, and bexarotene with carboplatin and paclitaxel in chemotherapy-naive patients with advanced or metastatic non-small-cell lung cancer: SPIRIT II. *J Clin Oncol*. 2008; 26:1879–1885. [PubMed: 18398153]
4. Kubota K, Kawahara M, Ogawara M, Nishiwaki Y, Komuta K, Minato K, et al. Vinorelbine plus gemcitabine followed by docetaxel versus carboplatin plus paclitaxel in patients with advanced non-small-cell lung cancer: a randomised, open-label, phase III study. *Lancet Oncol*. 2008; 9:1135–1142. [PubMed: 19013107]
5. Ramlau R, Zatloukal P, Jassem J, Schwarzenberger P, Orlov SV, Gottfried M, et al. Randomized phase III trial comparing bexarotene (L1069-49)/cisplatin/vinorelbine with cisplatin/vinorelbine in chemotherapy-naive patients with advanced or metastatic non-small-cell lung cancer: SPIRIT I. *J Clin Oncol*. 2008; 26:1886–1892. [PubMed: 18398154]
6. Scagliotti GV, Parikh P, von PJ, Biesma B, Vansteenkiste J, Manegold C, et al. Phase III study comparing cisplatin plus gemcitabine with cisplatin plus pemetrexed in chemotherapy-naive patients with advanced-stage non-small-cell lung cancer. *J Clin Oncol*. 2008; 26:3543–3551. [PubMed: 18506025]
7. Fidias PM, Dakhil SR, Lyss AP, Loesch DM, Waterhouse DM, Bromund JL, et al. Phase III study of immediate compared with delayed docetaxel after front-line therapy with gemcitabine plus carboplatin in advanced non-small-cell lung cancer. *J Clin Oncol*. 2009; 27:591–598. [PubMed: 19075278]
8. Pirker R, Pereira JR, Szczesna A, von PJ, Krzakowski M, Ramlau R, et al. Cetuximab plus chemotherapy in patients with advanced non-small-cell lung cancer (FLEX): an open-label randomised phase III trial. *Lancet*. 2009; 373:1525–1531. [PubMed: 19410716]
9. Folkman J. Tumor angiogenesis: therapeutic implications. *N Engl J Med*. 1971; 285:1182–1186. [PubMed: 4938153]
10. Ferrara N. VEGF and the quest for tumour angiogenesis factors. *Nat Rev Cancer*. 2002; 2:795–803. [PubMed: 12360282]
11. Ferrara N, Gerber HP, LeCouter J. The biology of VEGF and its receptors. *Nat Med*. 2003; 9:669–676. [PubMed: 12778165]
12. Ferrara N. Vascular endothelial growth factor: basic science and clinical progress. *Endocr Rev*. 2004; 25:581–611. [PubMed: 15294883]

13. Ferrara N. VEGF as a therapeutic target in cancer. *Oncology*. 2005; 69 (Suppl 3):11–16. [PubMed: 16301831]
14. Tammela T, Enholm B, Alitalo K, Paavonen K. The biology of vascular endothelial growth factors. *Cardiovasc Res*. 2005; 65:550–563. [PubMed: 15664381]
15. Olsson AK, Dimberg A, Kreuger J, Claesson-Welsh L. VEGF receptor signalling - in control of vascular function. *Nat Rev Mol Cell Biol*. 2006; 7:359–371. [PubMed: 16633338]
16. Ferrara N, Hillan KJ, Gerber HP, Novotny W. Discovery and development of bevacizumab, an anti-VEGF antibody for treating cancer. *Nat Rev Drug Discov*. 2004; 3:391–400. [PubMed: 15136787]
17. Ferrara N, Hillan KJ, Novotny W. Bevacizumab (Avastin), a humanized anti-VEGF monoclonal antibody for cancer therapy. *Biochem Biophys Res Commun*. 2005; 333:328–335. [PubMed: 15961063]
18. Presta LG, Chen H, O'Connor SJ, Chisholm V, Meng YG, Krummen L, et al. Humanization of an anti-vascular endothelial growth factor monoclonal antibody for the therapy of solid tumors and other disorders. *Cancer Res*. 1997; 57:4593–4599. [PubMed: 9377574]
19. Sweeney CJ, Miller KD, Sissons SE, Nozaki S, Heilman DK, Shen J, et al. The antiangiogenic property of docetaxel is synergistic with a recombinant humanized monoclonal antibody against vascular endothelial growth factor or 2-methoxyestradiol but antagonized by endothelial growth factors. *Cancer Res*. 2001; 61:3369–3372. [PubMed: 11309294]
20. Fox WD, Higgins B, Maiese KM, Drobnjak M, Cordon-Cardo C, Scher HI, et al. Antibody to vascular endothelial growth factor slows growth of an androgen-independent xenograft model of prostate cancer. *Clin Cancer Res*. 2002; 8:3226–3231. [PubMed: 12374693]
21. Watanabe M, Boyer JL, Hackett NR, Qiu J, Crystal RG. Genetic delivery of the murine equivalent of bevacizumab (avastin), an anti-vascular endothelial growth factor monoclonal antibody, to suppress growth of human tumors in immunodeficient mice. *Hum Gene Ther*. 2008; 19:300–310. [PubMed: 18324912]
22. Yang JC, Haworth L, Sherry RM, Hwu P, Schwartzentruber DJ, Topalian SL, et al. A randomized trial of bevacizumab, an anti-vascular endothelial growth factor antibody, for metastatic renal cancer. *N Engl J Med*. 2003; 349:427–434. [PubMed: 12890841]
23. Hurwitz H, Fehrenbacher L, Novotny W, Cartwright T, Hainsworth J, Heim W, et al. Bevacizumab plus irinotecan, fluorouracil, and leucovorin for metastatic colorectal cancer. *N Engl J Med*. 2004; 350:2335–2342. [PubMed: 15175435]
24. Miller KD, Chap LI, Holmes FA, Cobleigh MA, Marcom PK, Fehrenbacher L, et al. Randomized phase III trial of capecitabine compared with bevacizumab plus capecitabine in patients with previously treated metastatic breast cancer. *J Clin Oncol*. 2005; 23:792–799. [PubMed: 15681523]
25. Sandler A, Gray R, Perry MC, Brahmer J, Schiller JH, Dowlati A, et al. Paclitaxel-carboplatin alone or with bevacizumab for non-small-cell lung cancer. *N Engl J Med*. 2006; 355:2542–2550. [PubMed: 17167137]
26. Reck M, von PJ, Zatloukal P, Ramlau R, Gorbounova V, Hirsh V, et al. Phase III trial of cisplatin plus gemcitabine with either placebo or bevacizumab as first-line therapy for nonsquamous non-small-cell lung cancer: AVAIL. *J Clin Oncol*. 2009; 27:1227–1234. [PubMed: 19188680]
27. Watanabe M, Boyer JL, Crystal RG. Genetic delivery of bevacizumab to suppress vascular endothelial growth factor-induced high-permeability pulmonary edema. *Hum Gene Ther*. 2009; 20:598–610. [PubMed: 19254174]
28. Kim KJ, Li B, Houck K, Winer J, Ferrara N. The vascular endothelial growth factor proteins: identification of biologically relevant regions by neutralizing monoclonal antibodies. *Growth Factors*. 1992; 7:53–64. [PubMed: 1380254]
29. Baca, M.; Wells, JA., inventors. I. Genentech, assignee. Anti-VEGF antibodies. USA. 6,884,879. 1997.
30. Xiao X, Li J, Samulski RJ. Production of high-titer recombinant adeno-associated virus vectors in the absence of helper adenovirus. *J Virol*. 1998; 72:2224–2232. [PubMed: 9499080]
31. Rabinowitz JE, Rolling F, Li C, Conrath H, Xiao W, Xiao X, et al. Cross-packaging of a single adeno-associated virus (AAV) type 2 vector genome into multiple AAV serotypes enables transduction with broad specificity. *J Virol*. 2002; 76:791–801. [PubMed: 11752169]

32. Gao G, Vandenberghe LH, Alvira MR, Lu Y, Calcedo R, Zhou X, et al. Clades of Adeno-associated viruses are widely disseminated in human tissues. *J Virol.* 2004; 78:6381–6388. [PubMed: 15163731]
33. De BP, Heguy A, Hackett NR, Ferris B, Leopold PL, Lee J, et al. High levels of persistent expression of alpha1-antitrypsin mediated by the nonhuman primate serotype rh. 10 adeno-associated virus despite preexisting immunity to common human adeno-associated viruses. *Mol Ther.* 2006; 13:67–76. [PubMed: 16260185]
34. De BP, Hackett NR, Crystal RG, Boyer JL. Rapid/sustained anti-anthrax passive immunity mediated by co-administration of Ad/AAV. *Mol Ther.* 2008; 16:203–209. [PubMed: 18059375]
35. Plikaytis BD, Turner SH, Gheesling LL, Carlone GM. Comparisons of standard curve-fitting methods to quantitate *Neisseria meningitidis* group A polysaccharide antibody levels by enzyme-linked immunosorbent assay. *J Clin Microbiol.* 1991; 29:1439–1446. [PubMed: 1909345]
36. Rennard SI, Basset G, Lecossier D, O'Donnell KM, Pinkston P, Martin PG, et al. Estimation of volume of epithelial lining fluid recovered by lavage using urea as marker of dilution. *J Appl Physiol.* 1986; 60:532–538. [PubMed: 3512509]
37. Kaner RJ, Crystal RG. Compartmentalization of vascular endothelial growth factor to the epithelial surface of the human lung. *Mol Med.* 2001; 7:240–246. [PubMed: 11471568]
38. Gerber HP, Ferrara N. Pharmacology and pharmacodynamics of bevacizumab as monotherapy or in combination with cytotoxic therapy in preclinical studies. *Cancer Res.* 2005; 65:671–680. [PubMed: 15705858]
39. BenAmmar-Ceccoli S, Humblot S, Crouzier R, Acres B, Kieny MP, Herlyn D, et al. Recombinant vaccinia viruses expressing immunoglobulin variable regions efficiently and selectively protect mice against tumoral B-cell growth. *Cancer Gene Ther.* 2001; 8:815–826. [PubMed: 11687905]
40. Timmerman JM, Caspar CB, Lambert SL, Syrengelas AD, Levy R. Idiotype-encoding recombinant adenoviruses provide protective immunity against murine B-cell lymphomas. *Blood.* 2001; 97:1370–1377. [PubMed: 11222382]
41. Fang J, Qian JJ, Yi S, Harding TC, Tu GH, VanRoey M, et al. Stable antibody expression at therapeutic levels using the 2A peptide. *Nat Biotechnol.* 2005; 23:584–590. [PubMed: 15834403]
42. Jiang M, Shi W, Zhang Q, Wang X, Guo M, Cui Z, et al. Gene therapy using adenovirus-mediated full-length anti-HER-2 antibody for HER-2 overexpression cancers. *Clin Cancer Res.* 2006; 12:6179–6185. [PubMed: 17062695]
43. Ho DT, Wykoff-Clary S, Gross CS, Schneider D, Jin F, Kretschmer PJ, et al. Growth inhibition of an established A431 xenograft tumor by a full-length anti-EGFR antibody following gene delivery by AAV. *Cancer Gene Ther.* 2009; 16:184–194. [PubMed: 18758433]
44. Carter, BJ.; Burstein, H.; Peluso, RW. Adeno-associated virus and AAV vectors for gene delivery. In: Templeton, NS., editor. *Gene and cell therapy.* CRC Press; Boca Raton: 2008. p. 115
45. McCarty DM, Young SM Jr, Samulski RJ. Integration of adeno-associated virus (AAV) and recombinant AAV vectors. *Annu Rev Genet.* 2004; 38:819–845. [PubMed: 15568995]
46. De B, Heguy A, Leopold PL, Wasif N, Korst RJ, Hackett NR, et al. Intrapleural administration of a serotype 5 adeno-associated virus coding for alpha1-antitrypsin mediates persistent, high lung and serum levels of alpha1-antitrypsin. *Mol Ther.* 2004; 10:1003–1010. [PubMed: 15564132]
47. Skaricic D, Traube C, De B, Joh J, Boyer J, Crystal RG, et al. Genetic delivery of an anti-RSV antibody to protect against pulmonary infection with RSV. *Virology.* 2008; 378:79–85. [PubMed: 18556039]
48. Light, RW. Pleural effusions related to metastatic malignancies. In: Light, RW., editor. *Pleural diseases.* Lippincott Williams & Wilkins; Philadelphia: 2007. p. 133
49. Light, RW. Pneumothorax. In: Light, RW., editor. *Pleural diseases.* Lippincott Williams & Wilkins; Philadelphia: 2007. p. 306

**Figure 1.**

Expression and specificity of the anti-human VEGF mouse monoclonal antibody in cells infected with AAVrh.10αVEGF. **A.** AAVrh.10αVEGF production and secretion of heavy and light chains. 293orf6 cells were infected with AAVrh.10αVEGF or AAVrh.10EGFP at 2×10^5 genome copies (gc)/cell; mock-infected cells served as a negative control. Seventy-two hours postinfection, infected cell supernatants were assessed for anti-VEGF-A antibody expression by Western analysis with a horseradish peroxidase-conjugated sheep anti-mouse IgG antibody. Lane 1- supernatant from mock-infected cells; lane 2- AAVrh.10EGFP; lane 3- AAVrh.10αVEGF; and lane 4- purified mouse IgG1 positive control. The heavy and light chains of the antibody expressed by the Ad vector have molecular masses of 50 and 25 kDa, respectively. **B.** Human VEGF specificity of the anti-human VEGF-A antibody directed by AAVrh.10αVEGF. 293orf6 cells were infected with AAVrh.10EGFP or AAVrh.10αVEGF at 2×10^5 gc/cell. Seventy-two hours postinfection, infected cell supernatants were assessed for the ability to bind to human or mouse VEGF-A protein by Western analysis. Lanes 5–9, supernatants from AAVrh.10EGFP-infected cells. Lane 5- bovine serum albumin; lane 6- mouse VEGF-A120; lane 7- mouse VEGF-A164; lane 8- human VEGF-A121; and lane 9- human VEGF-A165. Lanes 10–14, AAVrh.10αVEGF-infected cells. Lane 10- bovine serum albumin; lane 11- mouse VEGF-A120; lane 12- mouse VEGF-A164; lane 13- human VEGF-A121; and lane 14- human VEGF-A165. Lanes 15–19, purified anti-human VEGF-A control. Lane 15- bovine serum albumin; lane 16- mouse VEGF-A120; lane 17- mouse VEGF-A164; lane 18- human VEGF-A121; and lane 19- human VEGF-A165. Human VEGF-A121 and VEGF-A165 have molecular masses of 14 and 19 kDa, respectively.

**Figure 2.**

Anti-VEGF-A antibody levels after local administration of the AAVrh.10αVEGF vector. **A.** Comparison of lung ELF anti-VEGF-A antibody levels after local administration of AAVrh.10αVEGF. AAVrh.10αVEGF (10^{11} gc) was administered to C57BL/6 mice by intrapleural (Ipl) or intratracheal (IT) route. AAVrh.10EGFP and AAVrh.10αPA were administered by the intrapleural route as controls. Eight weeks after vector administration, lung ELF anti-VEGF-A antibody levels were measured by human VEGF-A specific ELISA. Data were obtained from $n=5$ animals per group. **B.** Lung ELF and serum anti-VEGF-A antibody levels over 40 wk after intrapleural administration of AAVrh.10αVEGF. AAVrh.10EGFP and AAVrh.10αPA were administered by the intrapleural route as controls. Data were obtained from $n=4-5$ animals per group.

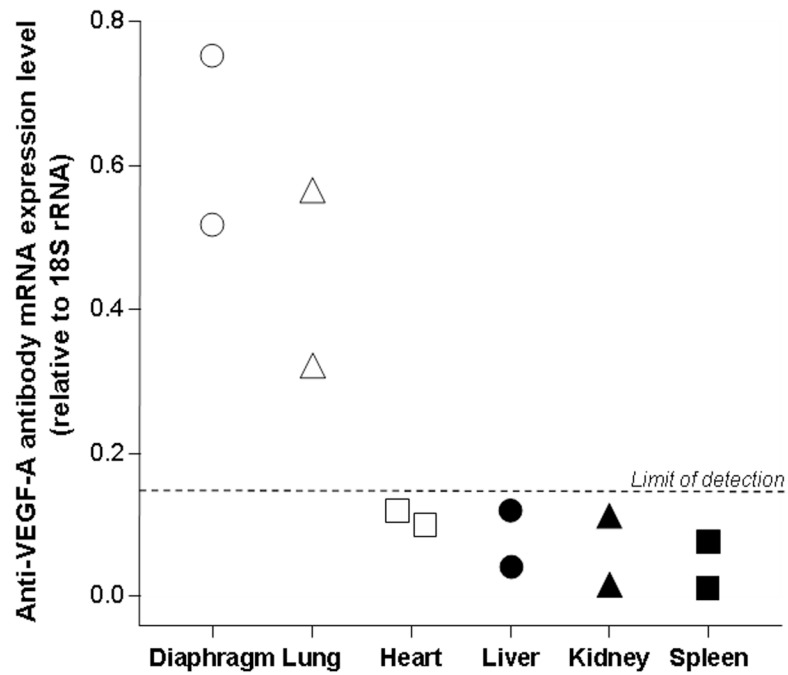


Figure 3.

Organ distribution of anti-VEGF-A antibody mRNA expression levels after intrapleural administration of AAVrh.10 α VEGF. AAVrh.10 α VEGF (10^{11} gc) was administered intrapleurally. At 18 wk, various organs were collected and anti-VEGF-A antibody mRNA expression levels relative to endogenous 18S rRNA were assessed by quantitative TaqMan real-time PCR (limit of detection, 0.15 relative to 18S rRNA). Data were obtained from n=2 animals per group.

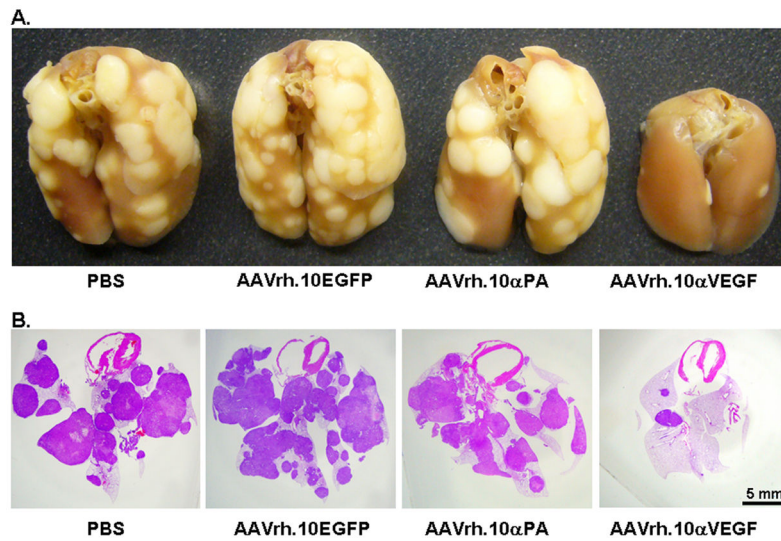


Figure 4. Lung metastatic tumors after intravenous administration of DU145 tumor cell and treatment with AAVrh10αVEGF. Tumor cells (5×10^5) were administered intravenously into NOD/SCID mice. On the next day, AAVrh.10αVEGF or control AAVrh.10αPA, AAVrh.10EGFP or PBS was administered by the intrapleural route (10^{11} gc). At 18 wk, lungs were fixed, photos were taken and paraffin sections were stained. **A.** Gross photos of lung under various conditions. **B.** Hematoxylin and eosin staining. Scale bar; 5 mm.

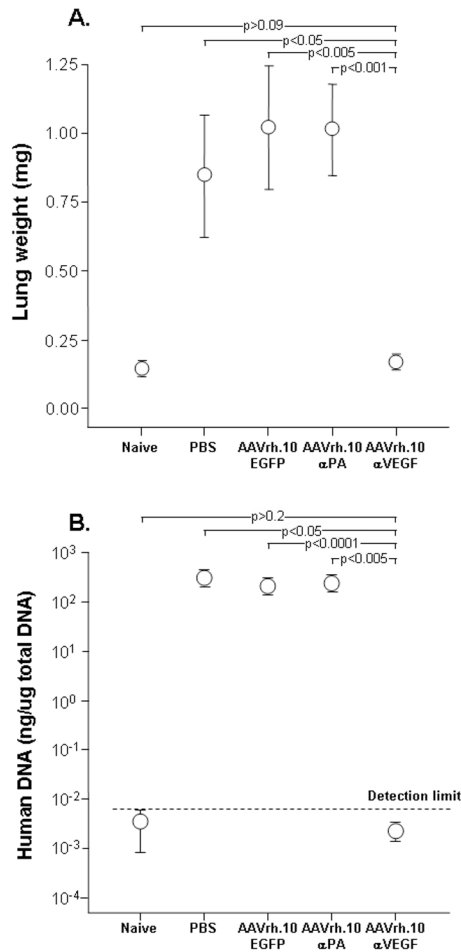


Figure 5.

Ability of AAVrh.10αVEGF to inhibit metastatic lung tumor growth. DU145 tumor cells (5×10^5) were administered intravenously into NOD/SCID mice. On the next day, mice were treated by intrapleural administration of 10^{11} gc AAVrh.10αVEGF or, as controls, AAVrh.10αPA, AAVrh.10EGFP or PBS. At 15 wk, lungs were collected, weighed and human *Alu* expression levels were assessed by quantitative TaqMan real-time PCR. Naive, n=3 animals per group. All other groups, n=4–5 animals per group. **A.** Lung weight; **B.** Tumor burden as assessed by human *Alu* TaqMan PCR with detection limit shown as a dotted line.

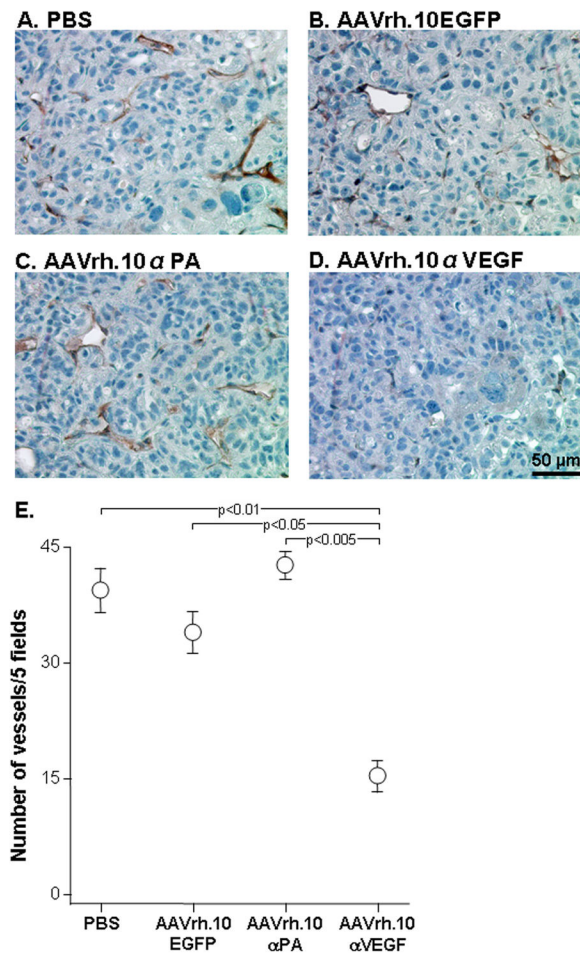


Figure 6. Ability of AAVrh.10αVEGF to inhibit metastatic lung tumor vascularization. DU145 tumor cells (5×10^5) were administered intravenously into NOD/SCID mice. On the next day, mice were treated by intrapleural administration of 10^{11} gc AAVrh.10αVEGF or, as controls, AAVrh.10αPA, AAVrh.10EGFP or PBS. At 18 wk, lungs were collected, and paraffin sections were stained using goat anti-mouse vascular endothelial cadherin (VE-cadherin) antibody, or isotype-matched control goat IgG followed by visualization with biotin-conjugated anti-goat IgG antibody, peroxidase conjugated streptavidin and diaminobenzidine. Nuclei were stained with hematoxylin. **A.** PBS; **B.** AAVrh.10EGFP; **C.** AAVrh.10αPA; **D.** AAVrh.10αVEGF; and **E.** Quantitation of the number of VE-cadherin⁺ vessels in metastatic lung tumor sections per 5 random fields. Data were obtained from n=3 animals per group. Scale bar: **A-D.** 50 μm.

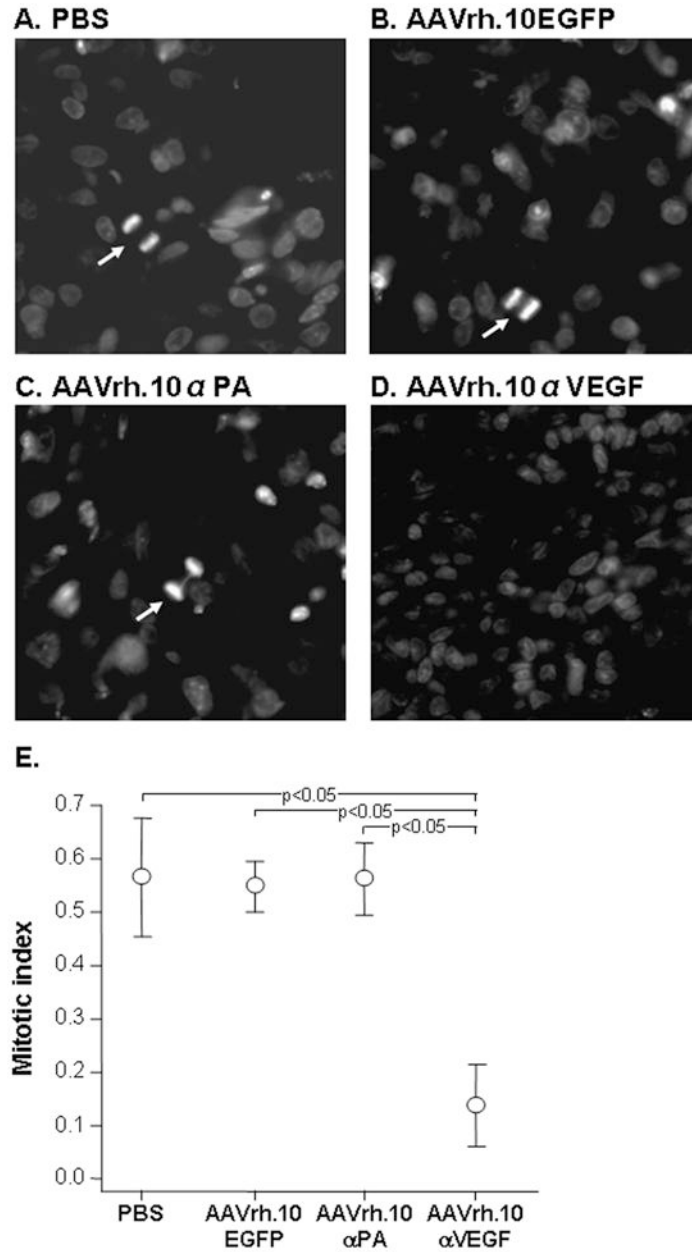


Figure 7.

Ability of AAVrh.10αVEGF to inhibit metastatic lung tumor proliferation. DU145 tumor cells (5×10^5) were administered intravenously into NOD/SCID mice. On the next day, mice were treated by intrapleural administration of 10^{11} gc AAVrh.10αVEGF or, as controls, AAVrh.10αPA, AAVrh.10EGFP or PBS. At 18 wk, lungs were collected, and nuclei were stained with 4',6-diamidino-2-phenylindole. **A–D.** DAPI stain. Mitotic nuclei noted with arrows. **A.** PBS; **B.** AAVrh.10EGFP; **C.** AAVrh.10αPA; **D.** AAVrh.10αVEGF; and **E.** Quantitation of the number of nuclei in mitotic phase in metastatic lung tumor sections per 5 random fields. Data were obtained from $n=3$ animals per group.

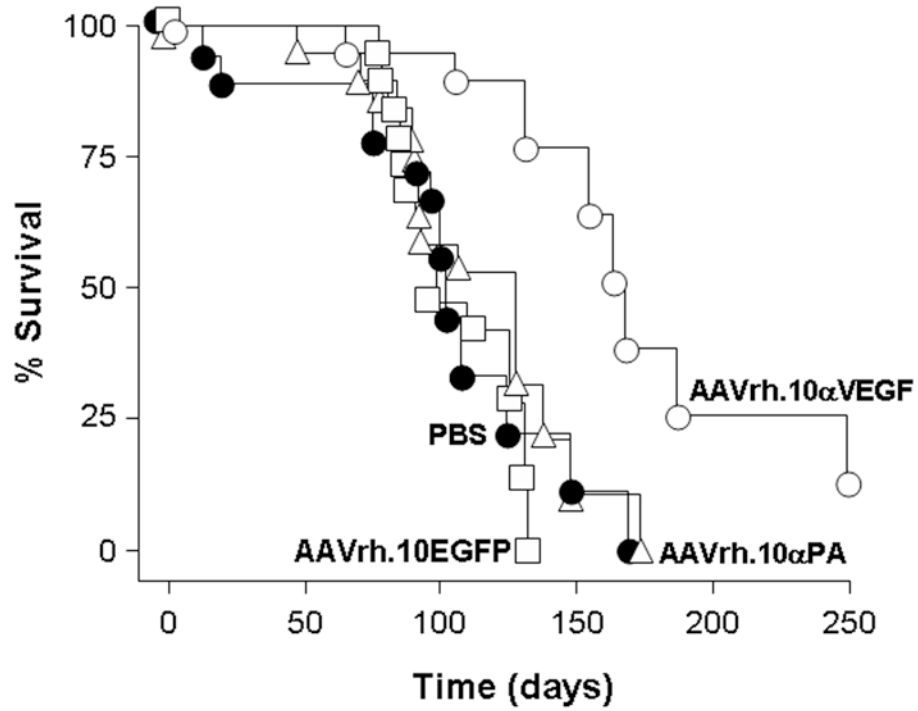


Figure 8.

Survival of AAVrh.10αVEGF-treated metastatic lung tumor-bearing mice. DU 145 tumor cells (5×10^5) were administered intravenously into NOD/SCID mice. On the next day, mice were treated by intrapleural administration of 10^{11} gc AAVrh.10αVEGF or, as controls, AAVrh.10αPA, AAVrh.10EGFP or PBS. Survival is presented as the percentage of surviving mice in each group. Data were obtained from $n=18-20$ animals per group. AAVrh.10αVEGF vs all other groups, $p < 0.002$.